



Contents lists available at ScienceDirect

LWT

journal homepage: www.elsevier.com/locate/lwt

Inactivation kinetics of *Bacillus cereus* vegetative cells and spores from different sources by antimicrobial photodynamic treatment (aPDT)

Leonardo do Prado-Silva^a, Verônica O. Alvarenga^{a,b}, Gilberto Ú.L. Braga^c, Anderson S. Sant'Ana^{a,*}

^a Department of Food Science and Nutrition, Faculty of Food Engineering, University of Campinas, Campinas, SP, Brazil

^b Department of Food, Faculty of Pharmacy - Federal University of Minas Gerais, Belo Horizonte, MG, Brazil

^c Department of Clinical, Toxicological and Bromatological Analysis, School of Pharmaceutical Sciences of Ribeirão Preto, University of São Paulo, Ribeirão Preto, SP, Brazil

ARTICLE INFO

Keywords:

Emerging technology
Nonthermal treatment
Pathogen
Spoilage
Phenothiazine dye

ABSTRACT

Antimicrobial photodynamic treatment (aPDT) is a promising alternative to conventional thermal inactivation methods. This study aimed to evaluate *Bacillus cereus* vegetative cells' inactivation and spores by aPDT with new methylene blue (NMB) as photosensitizer (PS) using red light. The efficacy of aPDT was determined initially by minimal inhibitory concentration (MIC) of NMB at different concentrations and fluences. Cluster analysis from the results of MIC grouped *B. cereus* strains according to their aPDT susceptibility. Then, four strains (B63, B3, 436, and ATCC 14579) were selected for a survival study of aPDT with NMB in three concentrations (5, 50, and 100 μM). The viability of *B. cereus* vegetative cells and spores was reduced in all tested fluences. The strain ATCC 14579 (vegetative cells and spores) was the most susceptible to aPDT at relatively low fluence (25 J/cm^2). The Weibull model presented a good fit for the inactivation data estimating the kinetic parameters δ (first decimal reduction) and p (shape parameter). This study contributes to the knowledge of the behavior of different strains of *B. cereus* regarding an emerging method of microbial inactivation. The variability of inactivation among strains will allow the development of more reliable processes.

1. Introduction

The contamination of foods with pathogens is responsible for mortality and morbidity that impact people's lives, countries' economies, and social development (WHO, 2015). According to the Center for Disease Control and Prevention (CDC) from the United States, 1 in 6 Americans gets sick from food poisoning each year (CDC, 2020). *Bacillus cereus* is a Gram-positive spore-forming rod-shaped bacterium commonly found in soil environments associated with foodborne illnesses and food spoilage (Spanu, 2016). Food poisonings caused by *B. cereus* is mainly characterized by vomiting (emetic toxin) and diarrhea (enterotoxin) (Bottone, 2010). In dairy products, *B. cereus* can also cause food spoilage by producing lipase, proteinase, and phospholipases that cause off-flavor, coagulation, and bitterness (Heyndrickx, 2011; Mehta, Metzger, Hassan, Nelson, & Patel, 2019; Spanu, 2016).

Food industries seek nonthermal and environmentally friendly alternatives to reduce or avoid the contamination of the products and, consequently, diminish foodborne diseases. Antimicrobial

photodynamic treatment (aPDT) is a promising technology that can effectively reduce microbial counts from the surface of foods and related materials (Gonzales et al., 2017; Luksiene, Buchovec, & Paskeviciute, 2009).

The microbial inactivation is mostly obtained through thermal and chemical treatment and controlled by good manufacturing, transportation, and storage practices. Even though conventional thermal methodologies are effective, it is known that they cause undesirable effects as losses in the sensory and nutritional quality of food (Barba, Koubaa, Prado-Silva, Orlien, & Sant'Ana, 2017; Uchida & Silva, 2017). Besides that, the use of chemical products as sanitizers is not considered environmentally friendly and harmful to humans (Ölmez & Kretschmar, 2009).

The mechanism of action of aPDT is based on the combination of three nontoxic components: visible light, oxygen, and a photosensitizer (PS). The visible light with the appropriate wavelength excites the PS molecule to a high-energy electronic state. This excited state reacts with the oxygen molecules nearby, producing reactive oxygen species (ROS)

* Corresponding author. Rua Monteiro Lobato 80, CEP 13083-862, Campinas, SP, Brazil.

E-mail address: and@unicamp.br (A.S. Sant'Ana).

<https://doi.org/10.1016/j.lwt.2021.111037>

Received 24 October 2020; Accepted 31 January 2021

Available online 2 February 2021

0023-6438/© 2021 Elsevier Ltd. This is an open access article under the CC BY-NC-ND license (<http://creativecommons.org/licenses/by-nc-nd/4.0/>).

such as singlet oxygen, superoxide, and radicals (Demidova & Hamblin, 2005). These cytotoxic compounds can oxidize many biomolecules, such as proteins, lipids, and nucleic acids, causing cell death (Almeida, Faustino, & Tomé, 2015; Brancini et al., 2016; Tonani et al., 2018; Žudyte & Lukšiene, 2019).

aPDT has been known since the mid-1900s as a treatment capable of reducing microbial counts after light exposition in the presence of dyes (Wainwright, 1998). Some studies have investigated the effect of different classes of PS as a well light source on the reduction of microbial contamination (Buchovec, Vaitonis, & Luksiene, 2009; Demidova & Hamblin, 2005; Le Marc, Buchovec, George, Baranyi, & Luksiene, 2009; Oliveira et al., 2009). It has been demonstrated the efficiency of aPDT with phenothiazinium dyes, such as toluidine blue O (TBO), methylene blue (MB), and new methylene blue (NMB), against *B. cereus* spores and vegetative cells (Demidova & Hamblin, 2005). Therefore, *B. cereus* comprises an interesting microorganism to be employed as a model for aPDT.

The current work aimed to evaluate the efficiency of aPDT using NMB and red light against *B. cereus* vegetative cells and spores from different sources. This study also estimated the aPDT inactivation kinetics for both forms of selected strains using the Weibull model. When possible, the fluence for 4D (fluence needed for four decimal reductions) was calculated.

2. Material and methods

2.1. Bacterial strains, cultivation, and preparation of spore suspensions

All strains of *B. cereus* ($n = 12$) used in this study were obtained from Fundação Oswaldo Cruz (Rio de Janeiro, Brazil). The strains used were isolated from the following sources: ATCC 14579 – “Standard strain”; 432 and 436 – “Chocolate”; 511, 512, 540 – “Dairy products”; B3 and B94 – “Milk”; B18 – “Starch”; B51 – “Meat”; B63 – “Ready meal”; and B86 – “Cornflour”. Cells were grown in nutrient broth (Kasvi, Italy) at 30 °C for 48 h; after centrifugation (Sorvall Legend XTR, Thermo Fisher Scientific, Waltham, MI, USA), the pure cells were stored at – 80 °C (Revco EXF, Thermo Fisher Scientific, Marietta, OH, USA) in cryotubes with 20% (w/w) glycerol until further use.

According to Pflug (1999), spore suspensions were prepared and confirmed by Alvarenga et al., 2018. Briefly, roux bottles were filled with approximately 200 mL of nutrient agar (Kasvi, Italy) supplemented with manganese sulfate (10 ppm) (Synth, Diadema, Brazil). After inoculation, the roux bottles were incubated at 30 °C for 30 days. The sporulation progress was frequently microscopically observed with malachite green staining to evaluate the spore formation. After such an incubation period, the suspensions were gently collected, scraping the agar surface with sterile deionized water followed by centrifugation (1500×g for 20 min at 4 °C). After five rounds of centrifugation, the spore suspensions were resuspended in sterile deionized water and heat-shocked (80 °C for 30 min) to kill any vegetative cells and enumerate the initial concentration of the spores and, finally, stored at – 20 °C until further use.

2.2. Photosensitizer

The phenothiazinium dye new methylene blue N zinc chloride double salt (NMB; Fig. 1) was purchased from Sigma-Aldrich, Inc. (St. Louis, MO, USA). A stock solution at the concentration of 500 µM was prepared

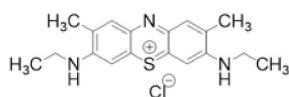


Fig. 1. Chemical structure of the new methylene blue (NMB) used as a photosensitizer in the study.

in phosphate-buffered saline (PBS; pH 7.4) and stored in the dark at –20 °C. Dilutions were prepared with PBS on the same day of the experiments.

2.3. Light source

The light was provided by an in-house-made array of 96 red light-emitting diodes (red LED96) with an emission peak at 631 nm. The measured irradiance from 400 to 700 nm was 24.50 mW/cm². Light measurements were performed according to de Menezes et al., 2016 using a cosine-corrected irradiance probe (CC-3-UV, Ocean Optics, Dunedin, FL, USA) screwed onto the end of an optical fiber coupled to a USB4000 spectroradiometer (Ocean Optics, Dunedin, FL, USA). Light intensity was measured inside the well to reduce external interference. This light source's choice was based on previous results obtained by the application of phenothiazinium photosensitizers and red light (Rodrigues, Ferreira, Wainwright, & Braga, 2012). The light source's emission spectrum can be seen in a previous publication (Rodrigues et al., 2012).

The fluences provided by the red LED96 calculated by Eq. (1):

$$f = I \times t \quad (1)$$

where, f = fluence in J/cm², I = irradiance in W/cm², and t = time of irradiation in s.

2.4. Antimicrobial photodynamic treatment

2.4.1. Evaluation of aPDT efficacies on vegetative cells of *B. cereus* based on the photosensitizer minimum inhibitory concentration (MIC)

The efficacy of aPDT with NMB combined with different fluences on vegetative cells of 12 strains of *B. cereus* was evaluated by determining the MIC of the PS at each fluence as previously described (Rodrigues et al., 2012). Briefly, 50 µL of the bacterial cell suspension ($\approx 10^5$ CFU/mL) and 50 µL of NMB were added to each well of sterile 96-well flat-bottomed plates (NEST Biotechnology, China). The final concentrations of NMB were 0, 1, 2.5, 5, 10, 12.5, 25, 50, 75, 100, and 200 µM. Plates were kept in the dark for 30 min at 30 °C and exposed to light fluences of 4.41 (3 min), 8.82 (6 min), 13.23 (9 min), and 22.05 J/cm² (15 min) using the red LED96 array as the light source (irradiance of 24.5 mW/cm²) or kept in the dark. The light and dark controls were performed to determine the effects of the light and NMB separately. After the exposures, 100 µL of nutrient broth (Kasvi, Italy) was added to each well followed the incubation of the plates at 30 °C for 48 h. MIC was considered the lowest PS concentration for each fluence, which inhibited the visible growth. Two independent experiments were performed in quadruplicate.

2.4.2. aPDT susceptibility of vegetative cells and spores of selected *B. cereus* strains

Vegetative cells from selected *B. cereus* strains (B3, B63,436, and ATCC 14579) were grown overnight in nutrient broth (Kasvi, Italy) at 30 °C and cell concentration was adjusted to 10^{6-8} CFU/mL in PBS using a McFarland turbidimeter (MS Tecnopon, Brazil). Spore suspensions of the selected strains at 10^7 spores/mL were prepared as previously described. Experiments were performed in 12-well flat-bottomed plates (NEST Biotechnology, China). Five mL of cell or spore suspensions and the solution of NMB were added to each well. The final concentrations of NMB were 5, 50, and 100 µM, which were selected based on previous MIC experiments. Plates were kept in the dark for 30 min at 30 °C before light exposition (24.5 mW/cm²). Vegetative cells and spores were illuminated for up to 120 min and 300 min, respectively. Aliquots of 100 µL were serially diluted, and the counts (CFU/mL) were determined by dropping onto nutrient agar (Kasvi, Italy) followed by overnight incubation at 30 °C. Three independent experiments were performed.

2.5. Modeling of aPDT inactivation data

Survival curves were obtained by plotting the logarithmical population counts (log CFU/mL or spores/mL) versus the fluence (J/cm^2). The inactivation data were analyzed by GlnaFit Excel® add-in, according to Geeraerd, Valdramidis, & Van Impe, 2005.

The Weibull model (Mafart, Couvert, Gaillard, & Leguerinel, 2002) was used with modifications according to Izquier & Gómez-López, 2011 (Eq. (2)):

$$\log_{10}N(t) = \log_{10}N(0) - \left(\frac{f}{\delta}\right)^p \quad (2)$$

where $N(t)$ (CFU/mL or spores/mL) is the number of survivors at the referred time, $N(0)$ (CFU/mL or spores/mL) is the initial population of vegetative cells or spores, f is the fluence (J/cm^2), δ (J/cm^2) is the fluency needed for the first decimal reduction, and p is the shape parameter (dimensionless) (Mafart et al., 2002).

2.6. Statistical analysis

All graphics and statistics were made using GraphPad Prism 6 (GraphPad Software, USA). To evaluate the differences between the conditions tested, the data were submitted to analysis of variance (ANOVA) followed by posthoc Tukey test. P values of <0.05 were considered significant. A cluster analysis was performed using Ward's algorithm of the ape package in software R, determining the Euclidean distance (Alvarenga et al., 2018).

3. Results and discussion

Given the importance of *B. cereus* commonly associated with food-borne illnesses, being also able to spoil food products (Mehta et al., 2019) in the present study were evaluated 12 different strains according to their susceptibility to aPDT. The efficacy of aPDT was firstly evaluated, determining the MIC for NMB at different fluences (4.41, 8.82, 13.23, and 22.05 J/cm^2). Exposure to red light in the absence of the PS did not inhibit the growth of any strain independent of the fluence used (data not shown). The dark control of the NMB at concentrations up to 200 μM did not inhibit the growth of any strain. The MIC of the NMB for all the fluences is depicted in Table 1. Only after 6 min of exposure corresponding to 8.82 J/cm^2 was possible to determine the MIC for all strains. The MIC varied among strains, and for most of them, it was possible to observe a decrease while fluence increases. The strain B63 was less susceptible to all fluences. The strains 432, B3, and B86 showed the same survival at fluences 4.41, 8.82, and 22.05 J/cm^2 . These strains

Table 1
Minimal inhibitory concentration of the NMB at concentrations from 0 to 200 μM illuminated by an array of 96 red light-emitting diodes (LED) at different fluences (J/cm^2).

| Strains | Source | Fluences (J/cm^2) | | | | |
|------------|------------|-----------------------|------|------|-------|-------|
| | | (Dark control) | 4.41 | 8.82 | 13.23 | 22.05 |
| 432 | Chocolate | >200 | 200 | 50 | 25 | 10 |
| 436 | | >200 | >200 | 75 | 25 | 10 |
| 511 | Dairy | >200 | >200 | 200 | 25 | 10 |
| 512 | products | >200 | >200 | 100 | 25 | 75 |
| 540 | | >200 | 75 | 25 | 10 | 5 |
| B3 | Milk | >200 | 200 | 50 | 50 | 10 |
| B94 | | >200 | 200 | 25 | 12.5 | 75 |
| B18 | Starch | >200 | 200 | 25 | 25 | 5 |
| B51 | Meat | >200 | 200 | 25 | 10 | 10 |
| B63 | Ready meal | >200 | 200 | 200 | 100 | 200 |
| B86 | Corn flour | >200 | 200 | 50 | 50 | 10 |
| ATCC 14579 | Standard | >200 | 200 | 25 | 75 | 12.5 |

survived in 200, 50, and 10 μM of NMB in the respective fluences. The strains B18, B51, B94, and ATCC 14579 (standard) presented the same MIC (25 μM) at 8.82 J/cm^2 .

According to the cluster analysis of such strains, two main groups could be observed based on their MIC (Fig. 2). The strains B63 (ready meal) and 511 (dairy products) were considered less susceptible. These strains survived in a concentration of 200 μM at fluences of 22.05 and 8.82 J/cm^2 , respectively. Four subgroups form the second group. The first subgroup (less susceptible) was composed of the strains B3 (milk), B86 (corn flour), and ATCC 14579 (standard strain) from different sources. These strains survived in a concentration of 200 μM at a fluence of 4.41 J/cm^2 . The second subgroup, composed of the strains 432 and 436 (chocolate) presenting the same MIC of 200 and 25 μM using fluences of 4.41 and 13.23 J/cm^2 , respectively. The third subgroup, composed of the strains B18 (starch), B51 (meat), and 540 (dairy products), presented the same MIC of 25 μM at fluences of 8.82 J/cm^2 . The fourth subgroup, B94 (milk) and 512 (dairy products), composed of the strains, were considered the most susceptible. These strains survived in concentrations of 25 and 12.5 μM , respectively, at a fluence of 13.23 J/cm^2 . The heterogeneity of the strains with different levels of aPDT susceptibility revealed a significative variability among the strains. This behavior was previously described by Alvarenga et al., 2018 with the same strains.

From the MIC results and the cluster analysis, 4 strains (B3, 436, B63, ATCC 14579) were selected according to their aPDT susceptibility. For such strains, the aPDT with NMB and the red light was conducted with vegetative cells and spores. The inactivation curves are presented as the log (N/N_0) of each strain to avoid small variation in the initial populations as a function of the fluence (J/cm^2).

As presented in Fig. 3, Fig. 4, the inactivation data of *B. cereus* vegetative cells and spores did not follow a log-linear inactivation in most cases. Therefore, the Weibull model with modifications (Izquier & Gómez-López, 2011) was used to fit inactivation data and estimate the aPDT inactivation kinetic parameters. From the Weibull model, it is possible to determine the δ -value, which was initially described by Mafart et al. (2002) as the time for first decimal reduction and adapted by Izquier and Gómez-López (2011) as the fluence (J/cm^2) needed for the first decimal reduction. Also, the Weibull model provides the p -value (shape parameter), which contributes to understanding microbial behavior. The R^2 obtained was higher than 0.87, indicating a good fit of the Weibull model to the data.

Fig. 3 shows the inactivation curves of the strains *B. cereus* vegetative cells submitted to aPDT. As expected, the less susceptible strain (B63; Fig. 3B) showed the lowest reduction in the viability at concentrations of 50 and 100 μM compared to the other strains ($P < 0.05$). At the same concentrations (50 and 100 μM), strains B3 (Figs. 3A), 436 (Fig. 3C), and ATCC 14579 (Fig. 3D) showed 4 and 5 log CFU/mL reductions when exposed to fluences of 73.50 and 88.20 J/cm^2 , respectively. For the most susceptible strain (ATCC 14579), it was only necessary 29.40 J/cm^2 , corresponding to 20 min of exposure to light, and 5 μM of NMB to achieve around 4 log CFU/mL reductions in cell viability. In previous studies, the viability of *B. cereus* was reduced by 4.4 log CFU/mL reductions after aPDT with the PS hypericin and approximately 40 min of light exposure (9.2 J/cm^2) (Aponiene, Paskeviciute, Reklaitis, & Luksiene, 2015). The use of 5-aminolevulinic acid (ALA) as a precursor of endogenous PSs at 3 and 7.5 mmol/L reduced *B. cereus*' viability from 4 to 6 log CFU/mL reductions (Le Marc et al., 2009). According to the authors, the efficiency of the aPDT depended on the fluence in agreement with the observed by the present study.

The spore inactivation required higher fluences than vegetative cells, which is expected given the less susceptibility structure, namely exosporium, developed during the sporulation process (Gerhardt & Ribi, 1964; Sanchez-Salas, Setlow, Zhang, Li, & Setlow, 2011). Nevertheless, during the spore inactivation of the most sensitive strain (ATCC 14579; Fig. 4D), the same fluence was necessary for vegetative cells (29.40 J/cm^2) achieve around 4 log spores/mL reductions. However, the

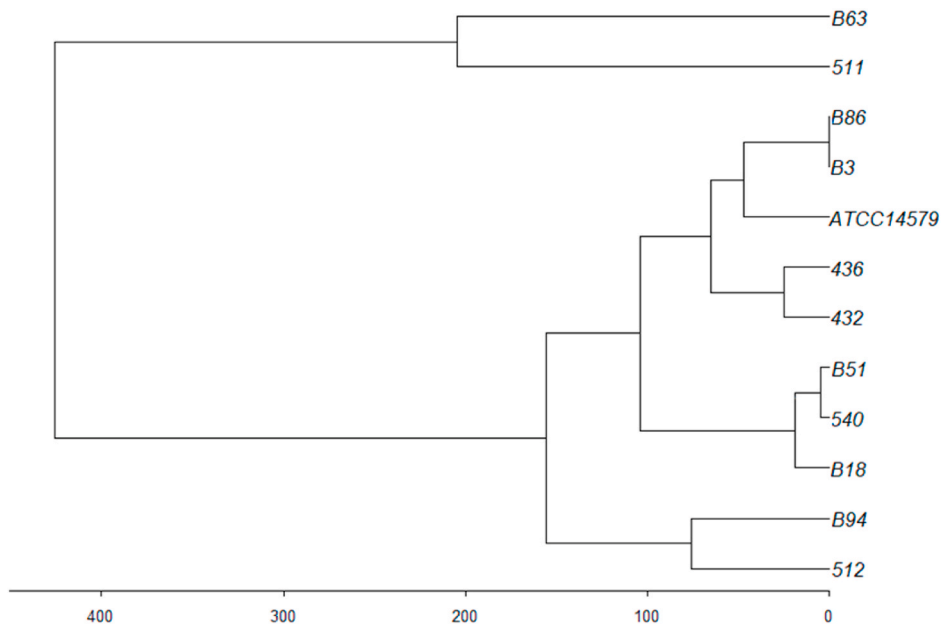


Fig. 2. Cluster analysis based on the MIC of *B. cereus* vegetative cells.

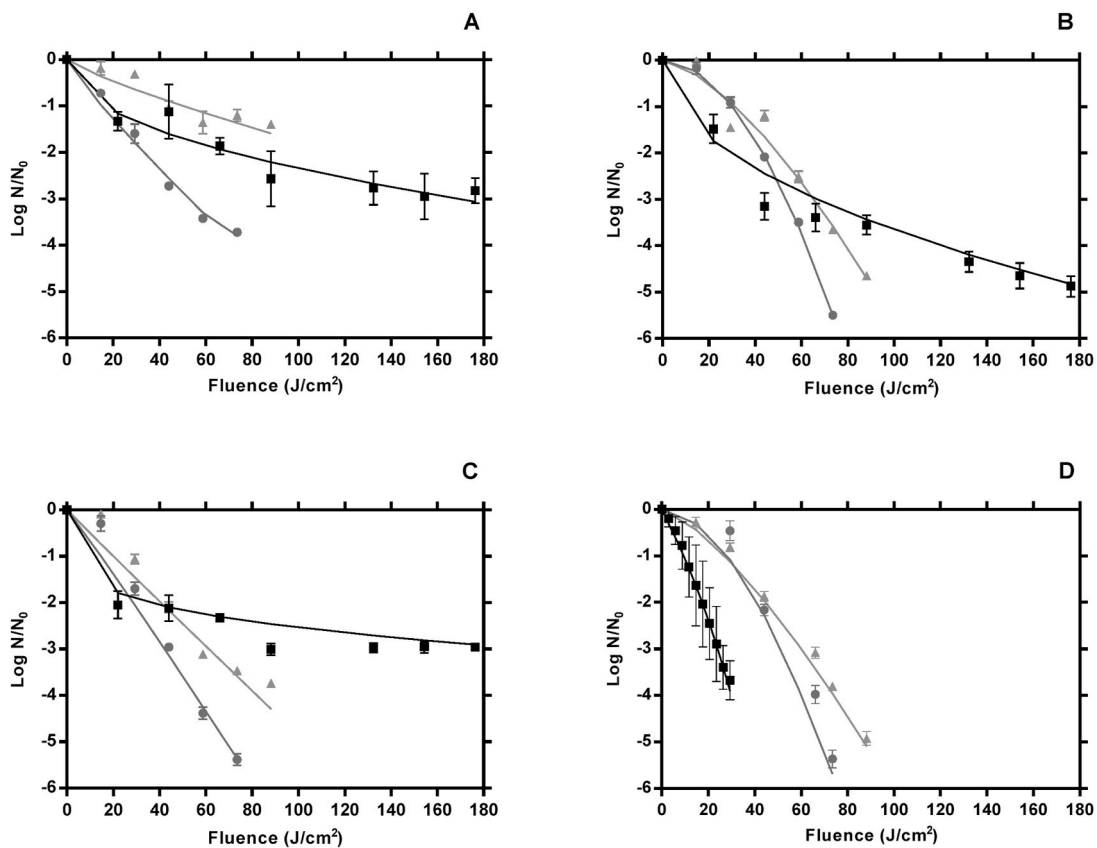


Fig. 3. aPDT inactivation curves of the vegetative cells of different strains of *B. cereus* – B63 (A), 436 (B), B3 (C), and ATCC 14579 (D) – in the presence of NMB at concentrations of ■ 5, ● 50, and ▲100 μM and different fluences (J/cm^2). All data correspond to three independent experiments. —: estimated curve by the Weibull model. Error bars represent the standard deviation (SD) of three independent experiments and, in some cases, are hidden by the symbols.

concentration required of NMB was higher (50 μM) than used for vegetative cells. A small difference in resistance between vegetative cells and *B. cereus* spores in PS concentration was previously cited by Demidova & Hamblin, 2005. The same authors also discussed the differential sensitivity of spores from *B. subtilis*, *B. atrophaeus*, and *B. megaterium*

(Demidova & Hamblin, 2005). A large difference in terms of aPDT susceptibility was detected between *B. cereus/B. thuringiensis* and *B. megaterium*, which the authors attribute to a structural difference in the spores. The exosporium present in the species *B. cereus/B. thuringiensis* and not in the *B. megaterium* can contribute to the accumulation

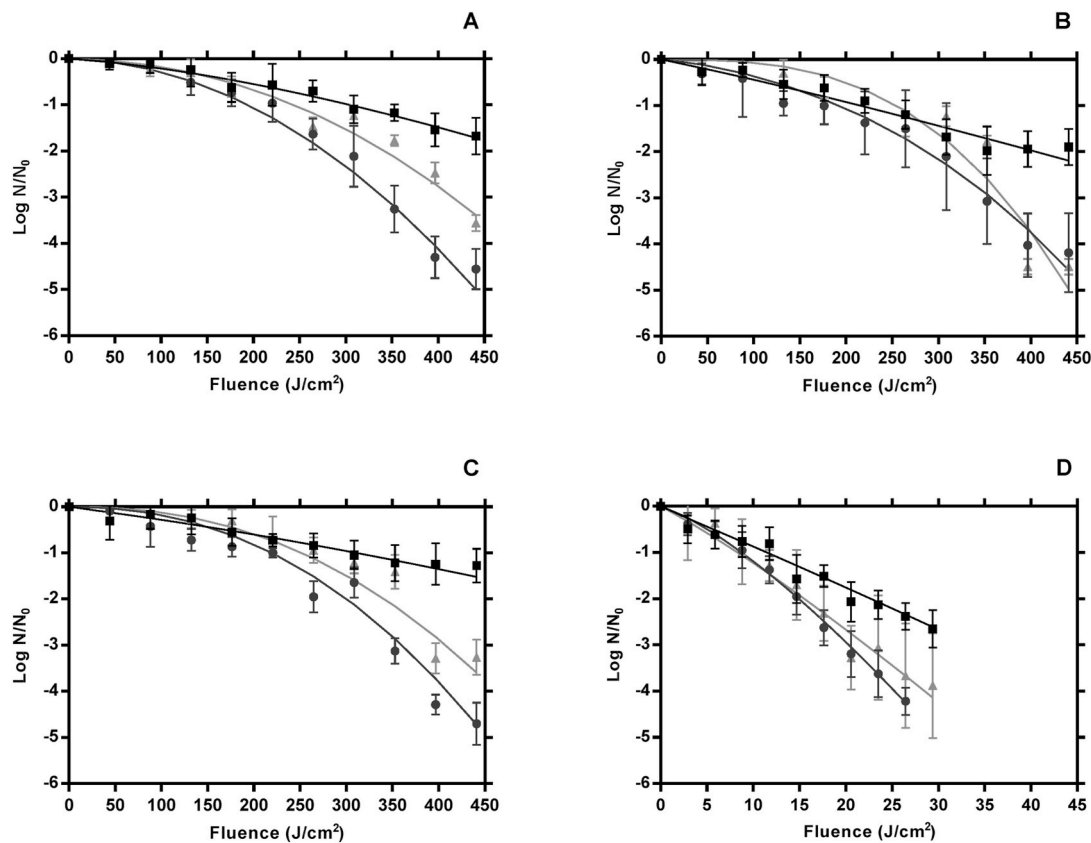


Fig. 4. aPDT inactivation curves of the spores of different strains of *B. cereus* – B63 (A), 436 (B), B3 (C), and ATCC 14579 (D) – in the presence of NMB at concentrations of ■ 5, ● 50, and ▲100 μM and different fluences (J/cm^2). All data correspond to three independent experiments. —: estimated curve by the Weibull model. Error bars represent the standard deviation (SD) of three independent experiments and, in some cases, are hidden by the symbols.

of PS, allowing the dye's diffusion inside the spore (Demidova & Hamblin, 2005).

The strains B3, B63, and 436 (Fig. 4 A-B-C, respectively) presented similar inactivation curves at all NMB concentrations and fluences. Such less susceptible behavior of these strains was also detected during the spray drying process, where the strain B63 was classified with intermediate susceptibility and the strains 436 and B3 as less susceptible to the process (Alvarenga et al., 2018). The same authors explored the differences in heat stress tolerance among different *B. cereus* strains at the molecular level with proteomic analysis. The results indicated that the observed variability between *B. cereus* strains could be related to spore coat protein expression (Alvarenga et al., 2018). There are no studies in the literature explaining the variability between *B. cereus* strains related to aPDT, which presents different inactivation mechanisms compared to thermal processes.

Photoinactivation of *B. cereus* spores mediated by ALA-based, porphyrin derivatives, phenothiazinium dyes, and hypericin-based PS showed significant inactivation results from approximately 2.5 to 6.0 log CFU/mL reductions (Dementavicius, Lukseviciute, Gómez-López, & Luksiene, 2016; Demidova & Hamblin, 2005; Luksiene et al., 2009; Oliveira et al., 2009). TBO is a phenothiazinium dye frequently used for PDT of bacteria and fungi (Demidova & Hamblin, 2005; Gonzales, Da Silva, Roberts, & Braga, 2010; Mahmoudi, Pourhajibagher, Alikhani, & Bahador, 2019). Since TBO had presented promising results of *B. cereus* spores inactivation, other types of phenothiazinium dyes were evaluated, including NMB (Demidova & Hamblin, 2005). In that study, photoinactivation of *B. cereus* spores mediated by NMB at 50 μM achieved more than 5 log CFU/mL reductions with half of the fluence used with TBO (40 J/cm^2) (Demidova & Hamblin, 2005). It is necessary to consider the incubation time of the PS of 3 h as opposed to 30 min in our study. It is also essential to highlight the spores' age significantly

different from 30 days in our study and 3 days declared by Demidova and Hamblin (2005). Such discrepancy in the spore maturation may explain the difference between the present study and the literature (Dementavicius et al., 2016; Demidova & Hamblin, 2005; Luksiene et al., 2009; Oliveira et al., 2009).

Tables 2 and 3 gives the fitted photodynamic inactivation kinetics parameters (δ and p -values) of vegetative cells and spores of the *B. cereus* strains using the Weibull model. As depicted in Table 2, the highest and smallest δ value (J/cm^2) was found for the strain B63 (50.24 ± 5.21) and B3 (0.51 ± 0.30) with NMB at 100 and 5 μM , respectively ($P < 0.05$). The highest δ values of the strains 436 and ATCC 14579 did not differ significantly at 50 and 100 μM ($P < 0.05$). Most of the lowest δ values were observed with NMB at 5 μM , suggesting that the minimum concentration of NMB binds quickly to the cell membrane causing fast inactivation. However, according to the p values presented in Table 2, the strains B3, B63, and 436 become less affected as the fluence increase with NMB 5 μM . This is confirmed by Fig. 3-A-B-C, which clearly shows an upward concavity ($p < 1$) of the curves. The only strain with $p > 1$ (downward concavity) for all concentrations of NMB was the ATCC 14579, which indicates that the cells are progressively killed in all conditions. The Weibull model described the photoinactivation mediated by ALA of *B. cereus* spores with linear, downward, and upward concavity shapes of the inactivation curves (Le Marc et al., 2009). In that study, the authors suggest that the incubation time and concentration of PS impact the p -value, increasing the inactivation in the first minutes, although remaining cells become less affected (Le Marc et al., 2009).

In all conditions tested for *B. cereus* spores, p values were >1 (Table 3). The downward concavity ($p > 1$) indicates that the microorganisms become increasingly damaged (Van Boekel, 2002). Such behavior can be confirmed by the δ values in all *B. cereus* spore inactivation conditions, except in the case of the strain ATCC 14579. Among

Table 2

Photoinactivation kinetic parameters of aPDT obtained from Weibull modeling for *B. cereus* vegetative cells.

| Strains | NMB (μM) | δ (mean \pm SD) (J/cm^2) | p -value (mean \pm SD) | 4D (mean \pm SD) (J/cm^2) | R^2 |
|------------|-----------------------|---|-------------------------------|---|-------|
| B3 | 5 | 0.51 \pm 0.30 ^{cC} | 0.21 \pm 0.06 ^{cB} | ND | 0.96 |
| | 50 | 14.81 \pm 0.62 ^{bC} | 1.05 \pm 0.02 ^{aC} | 56.01 \pm 1.45 ^{bD} | 0.98 |
| | 100 | 20.17 \pm 1.15 ^{aC} | 0.99 \pm 0.03 ^{bC} | 82.61 \pm 1.33 ^{aA} | 0.96 |
| B63 | 5 | 16.01 \pm 5.15 ^{bA} | 0.46 \pm 0.09 ^{bB} | ND | 0.90 |
| | 50 | 15.32 \pm 1.36 ^{bC} | 0.89 \pm 0.05 ^{aB} | 72.76 \pm 0.46 ^D | 0.98 |
| | 100 | 50.24 \pm 5.21 ^{aA} | 0.83 \pm 0.13 ^{aD} | ND | 0.87 |
| 436 | 5 | 7.67 \pm 3.75 ^{bB} | 0.49 \pm 0.06 ^{cB} | 121.42 \pm 14.82 ^{aA} | 0.96 |
| | 50 | 30.50 \pm 0.29 ^{aA} | 1.94 \pm 0.01 ^{aA} | 62.60 \pm 0.55 ^{cB} | 0.99 |
| | 100 | 31.62 \pm 1.16 ^{aB} | 1.51 \pm 0.04 ^{bA} | 79.38 \pm 0.92 ^{bB} | 0.97 |
| ATCC 14579 | 5 | 10.54 \pm 5.53 ^b | 1.40 \pm 0.57 ^{aA} | 26.46 \pm 0.00 ^{cB} | 0.99 |
| | 50 | 28.21 \pm 1.70 ^{aB} | 1.84 \pm 0.11 ^{aA} | 60.39 \pm 1.18 ^{bC} | 0.98 |
| | 100 | 27.05 \pm 1.62 ^{aB} | 1.38 \pm 0.08 ^{aB} | 74.68 \pm 0.72 ^{aC} | 0.99 |

δ : fluence needed for the first decimal reduction.

p -value: shape parameter (dimensionless).

4D: fluence needed to achieve four log reductions.

R^2 : determination coefficient.

Different lowercase letters in the same column within each strain (B3, B63, 436, and ATCC 14579) indicate significant difference in inactivation kinetic parameters ($P < 0.05$) according to one-way ANOVA followed by post-hoc Tukey test. Different uppercase letters in the same column within each concentration of NMB (5, 50, and 100 μM) indicate significant difference in inactivation kinetic parameters ($P < 0.05$) according to one-way ANOVA followed by post-hoc Tukey test.

the strains B3, B63, and 436, the smallest and highest δ values (196.23 \pm 32.27 and 296.88 \pm 66.86) were observed for B63 and B3 with NMB at 50 and 5 μM , respectively. δ values for the strain ATCC 14579 were significantly different in all conditions ($P > 0.05$). Also, the fluence of four decimal reductions (4D) for all strains tested to come up to 400 J/cm^2 at 50 μM of NMB, except for the strain ATCC 14579 with 25 J/cm^2 at 50 and 100 μM . The spore inactivation kinetic parameters (especially, δ value) of the strain ATCC 14579 (Table 3) confirm that this microorganism has high susceptibility to the aPDT compared to the other strains.

This study evaluated for the first time the effect of aPDT against *B. cereus* strains from different sources. The use of aPDT with NMB and the red light reduced *B. cereus* in both forms (vegetative cells and spores). The variability among strains of *B. cereus* represents a significant challenge for food safety. Also, the results of this study indicated that the strain ATCC 14579, widely used as the standard for thermal processing, was the most susceptible to aPDT. Further studies are needed to explain how the variability among strains of the same species occurs. The Weibull model successfully described a non-log-linear photoinactivation of vegetative cells and spores of *B. cereus* as well as the estimation of the kinetic parameters. The mathematical modeling can be a useful tool to determine the ideal conditions for photodynamic inactivation and assist a feasible implementation of aPDT by the industry.

Table 3

Photoinactivation kinetic parameters of aPDT obtained from Weibull modeling of *B. cereus* spores.

| Strains | NMB (μM) | δ (mean \pm SD) (J/cm^2) | p -value (mean \pm SD) | 4D (mean \pm SD) (J/cm^2) | R^2 |
|------------|-----------------------|---|--------------------------------|---|-------|
| B3 | 5 | 296.88 \pm 66.86 ^{aA} | 1.25 \pm 0.37 ^b | ND | 0.94 |
| | 50 | 219.61 \pm 12.05 ^{bA} | 2.24 \pm 0.27 ^{aA} | 413.07 \pm 10.10 ^A | 0.95 |
| | 100 | 251.67 \pm 11.42 ^{abA} | 2.29 \pm 0.20 ^{aB} | ND | 0.91 |
| B63 | 5 | 309.07 \pm 56.83 ^{aA} | 1.50 \pm 0.32 ^{bA} | ND | 0.88 |
| | 50 | 196.23 \pm 32.27 ^{bA} | 2.02 \pm 0.38 ^{aA} | 395.92 \pm 18.55 ^A | 0.98 |
| | 100 | 243.54 \pm 27.57 ^{bA} | 2.10 \pm 0.39 ^{aB} | ND | 0.91 |
| 436 | 5 | 222.57 \pm 42.78 ^{aB} | 1.09 \pm 0.18 ^{cB} | ND | 0.89 |
| | 50 | 202.66 \pm 69.15 ^{aA} | 2.13 \pm 0.89 ^{bA} | 400.05 \pm 36.01 ^{aA} | 0.94 |
| | 100 | 255.20 \pm 14.10 ^{aA} | 2.95 \pm 0.32 ^{aA} | 411.13 \pm 1.93 ^{aA} | 0.90 |
| ATCC 14579 | 5 | 11.57 \pm 2.50 ^{aC} | 1.04 \pm 0.18 ^{bB} | ND | 0.92 |
| | 50 | 8.87 \pm 1.70 ^{bB} | 1.33 \pm 0.20 ^{aB} | 24.96 \pm 1.15 ^{aB} | 0.98 |
| | 100 | 8.56 \pm 1.59 ^{bB} | 1.11 \pm 0.21 ^{abC} | 25.09 \pm 0.70 ^{aB} | 0.93 |

δ : fluence needed for the first decimal reduction.

p -value: shape parameter (dimensionless).

4D: fluence needed to achieve four log reductions.

R^2 : determination coefficient.

Different lowercase letters in the same column within each strain (B3, B63, 436, and ATCC 14579) indicate significant difference in inactivation kinetic parameters ($P < 0.05$) according to one-way ANOVA followed by post-hoc Tukey test. Different uppercase letters in the same column within each concentration of NMB (5, 50, and 100 μM) indicate significant difference in inactivation kinetic parameters ($P < 0.05$) according to one-way ANOVA followed by post-hoc Tukey test.

Declaration of competing interest

The authors declare that they have no known competing financial interests or personal relationships that could have appeared to influence the work reported in this paper.

Acknowledgment

This work was supported by: Conselho Nacional de Desenvolvimento Científico e Tecnológico (CNPq) (Grants #140092/2017–0, #302763/2014–7, and #305804/2017–0); Coordenação de Aperfeiçoamento de Pessoal de Nível Superior (CAPES) - Finance Code001 for the financial support.

References

- Almeida, A., Faustino, M. A. F., & Tomé, J. P. C. (2015). Photodynamic inactivation of bacteria: Finding effective targets. *Future Medicinal Chemistry*, 7(10), 1221–1224. <https://doi.org/10.4155/fmc.15.59>
- Alvarenga, V. O., Brancini, G. T. P., Silva, E. K., da Pia, A. K. R., Campagnollo, F. B., Braga, G. Ú. L., et al. (2018). Survival variability of 12 strains of *Bacillus cereus* yielded spray drying of whole milk. *International Journal of Food Microbiology*, 286, 80–89. <https://doi.org/10.1016/j.ijfoodmicro.2018.07.020>
- Aponiène, K., Paskėviciute, E., Reklaitis, I., & Luksiene, Z. (2015). Reduction of microbial contamination of fruits and vegetables by hypericin-based photosensitization: Comparison with other emerging antimicrobial treatments. *Journal of Food Engineering*, 144, 29–35. <https://doi.org/10.1016/j.jfoodeng.2014.07.012>
- Barba, F. J., Koubaa, M., Prado-Silva, L., Orlien, V., & Sant'Ana, A. S. (2017). Mild processing applied to the inactivation of the main foodborne bacterial pathogens: A

- review. *Trends in Food Science & Technology*, 66, 20–35. <https://doi.org/10.1016/j.tifs.2017.05.011>
- Bottone, E. J. (2010). *Bacillus cereus*, a volatile human pathogen. *Clinical Microbiology Reviews*, 23(2), 382–398. <https://doi.org/10.1128/CMR.00073-09>
- Brancini, G. T. P., Rodrigues, G. B., Rambaldi, M. D. S. L., Izumi, C., Yatsuda, A. P., Wainwright, M., et al. (2016). The effects of photodynamic treatment with new methylene blue N on the: *Candida albicans* proteome. *Photochemical and Photobiological Sciences*, 15(12), 1503–1513. <https://doi.org/10.1039/c6pp00257a>
- Buchovec, I., Vaitonis, Z., & Luksiene, Z. (2009). Novel approach to control *Salmonella enterica* by modern biophotonic technology: Photosensitization. *Journal of Applied Microbiology*, 106(3), 748–754. <https://doi.org/10.1111/j.1365-2672.2008.03993.x>
- Cdc. (2020). Food safety. Center for Disease control and prevention. <https://www.cdc.gov/foodsafety/index.html>. (Accessed 23 February 2020).
- Dementavicius, D., Lukseviciute, V., Gómez-López, V. M., & Luksiene, Z. (2016). Application of mathematical models for bacterial inactivation curves using Hypericin-based photosensitization. *Journal of Applied Microbiology*, 120(6), 1492–1500. <https://doi.org/10.1111/jam.13127>
- Demidova, T. N., & Hamblin, M. R. (2005). Photodynamic inactivation of *Bacillus* spores, mediated by phenothiazinium dyes. *Applied and Environmental Microbiology*, 71(11), 6918–6925. <https://doi.org/10.1128/AEM.71.11.6918>
- Geeraerd, A. H., Valdramidis, V. P., & Van Impe, J. F. (2005). GInaFIT, a freeware tool to assess non-log-linear microbial survivor curves. *International Journal of Food Microbiology*, 102(1), 95–105. <https://doi.org/10.1016/j.ijfoodmicro.2004.11.038>
- Gerhardt, P., & Ribí, E. (1964). Ultrastructure of the exosporium enveloping spores of *Bacillus cereus*. *Journal of Bacteriology*, 88(6), 1774–1789. <https://doi.org/10.1128/jb.88.6.1774-1789.1964>
- Gonzales, J. C., Brancini, G. T. P., Rodrigues, G. B., Silva-Junior, G. J., Bachmann, L., Wainwright, M., et al. (2017). Photodynamic inactivation of conidia of the fungus *Colletotrichum abscessum* on *Citrus sinensis* plants with methylene blue under solar radiation. *Journal of Photochemistry and Photobiology B: Biology*, 176, 54–61. <https://doi.org/10.1016/j.jphotobiol.2017.09.008>
- Gonzales, F. P., Da Silva, S. H., Roberts, D. W., & Braga, G. U. L. (2010). Photodynamic inactivation of conidia of the fungi *Metarhizium anisopliae* and *Aspergillus nidulans* with methylene blue and toluidine blue. *Photochemistry and Photobiology*, 86(3), 653–661. <https://doi.org/10.1111/j.1751-1097.2009.00689.x>
- Heyndrickx, M. (2011). The importance of endospore-forming bacteria originating from soil for contamination of industrial food processing. *Applied and Environmental Soil Science*, 1–11. <https://doi.org/10.1155/2011/561975>, 2011.
- Izquier, A., & Gómez-López, V. M. (2011). Modeling the pulsed light inactivation of microorganisms naturally occurring on vegetable substrates. *Food Microbiology*, 28(6), 1170–1174. <https://doi.org/10.1016/j.fm.2011.03.010>
- Le Marc, Y., Buchovec, I., George, S. M., Baranyi, J., & Luksiene, Z. (2009). Modelling the photosensitization-based inactivation of *Bacillus cereus*. *Journal of Applied Microbiology*, 107(3), 1006–1011. <https://doi.org/10.1111/j.1365-2672.2009.04275.x>
- Luksiene, Z., Buchovec, I., & Paskeviciute, E. (2009). Inactivation of food pathogen *Bacillus cereus* by photosensitization in vitro and on the surface of packaging material. *Journal of Applied Microbiology*, 107(6), 2037–2046. <https://doi.org/10.1111/j.1365-2672.2009.04383.x>
- Mafart, P., Couvert, O., Gaillard, S., & Leguerinel, I. (2002). On calculating sterility in thermal preservation methods: Application of the Weibull frequency distribution model. *International Journal of Food Microbiology*, 72, 107–113. [https://doi.org/10.1016/S0168-1605\(01\)00742-5](https://doi.org/10.1016/S0168-1605(01)00742-5)
- Mahmoudi, H., Pourhajibagher, M., Alikhani, M. Y., & Bahador, A. (2019). The effect of antimicrobial photodynamic therapy on the expression of biofilm associated genes in *Staphylococcus aureus* strains isolated from wound infections in burn patients. *Photodiagnosis and Photodynamic Therapy*, 25, 406–413. <https://doi.org/10.1016/j.pdpdt.2019.01.028>
- Mehta, D. S., Metzger, L. E., Hassan, A. N., Nelson, B. K., & Patel, H. A. (2019). The ability of spore formers to degrade milk proteins, fat, phospholipids, common stabilizers, and exopolysaccharides. *Journal of Dairy Science*, 102(12), 10799–10813. <https://doi.org/10.3168/jds.2019-16623>
- de Menezes, H. D., Tonani, L., Bachmann, L., Wainwright, M., Braga, G. Ú. L., & von Zeska Kress, M. R. (2016). Photodynamic treatment with phenothiazinium photosensitizers kills both ungerminated and germinated microconidia pathogenic fungi *Fusarium oxysporum*, *Fusarium moniliforme*, and *Fusarium solani*. *Journal of Photochemistry and Photobiology B: Biology*, 164, 1–12. <https://doi.org/10.1016/j.jphotobiol.2016.09.008>
- Oliveira, A., Almeida, A., Carvalho, C. M. B., Tomé, J. P. C., Faustino, M. A. F., Neves, M. G. P. M. S., et al. (2009). Porphyrin derivatives as photosensitizers for the inactivation of *Bacillus cereus* endospores. *Journal of Applied Microbiology*, 106(6), 1986–1995. <https://doi.org/10.1111/j.1365-2672.2009.04168.x>
- Ölmez, H., & Kretzschmar, U. (2009). Potential alternative disinfection methods for organic fresh-cut industry for minimizing water consumption and environmental impact. *Lebensmittel-Wissenschaft und -Technologie- Food Science and Technology*, 42(3), 686–693. <https://doi.org/10.1016/j.lwt.2008.08.001>
- Rodrigues, G. B., Ferreira, L. K. S., Wainwright, M., & Braga, G. U. L. (2012). Journal of Photochemistry and Photobiology B: Biology Susceptibilities of the dermatophytes *Trichophyton mentagrophytes* and *T. rubrum* microconidia to photodynamic antimicrobial chemotherapy with novel phenothiazinium photosensitizers and red light. *Journal of Photochemistry and Photobiology B: Biology*, 116, 89–94. <https://doi.org/10.1016/j.jphotobiol.2012.08.010>
- Sanchez-Salas, J. L., Setlow, B., Zhang, P., Li, Y. Q., & Setlow, P. (2011). Maturation of released spores is necessary for acquisition of full spore heat resistance during *Bacillus subtilis* sporulation. *Applied and Environmental Microbiology*, 77(19), 6746–6754. <https://doi.org/10.1128/AEM.05031-11>
- Spanu, C. (2016). Sporeforming bacterial pathogens in ready-to-eat dairy products. In *Food hygiene and toxicology in ready-to-eat foods*. <https://doi.org/10.1016/B978-0-12-801916-0.00015-7>
- Tonani, L., Morosini, N. S., Dantas de Menezes, H., Nadaletto Bonifácio da Silva, M. E., Wainwright, M., Leite Braga, G. Ú., et al. (2018). In vitro susceptibilities of *Neoscytalidium* spp. sequence types to antifungal agents and antimicrobial photodynamic treatment with phenothiazinium photosensitizers. *Fungal Biology*, 122(6), 436–448. <https://doi.org/10.1016/j.funbio.2017.08.009>
- Uchida, R., & Silva, F. V. M. (2017). *Alicyclobacillus acidoterrestris* spore inactivation by high pressure combined with mild heat: Modeling the effects of temperature and soluble solids. *Food Control*, 73, 426–432. <https://doi.org/10.1016/j.foodcont.2016.08.034>
- Van Boekel, M. A. J. S. (2002). On the use of the Weibull model to describe thermal inactivation of microbial vegetative cells. *International Journal of Food Microbiology*, 74(1–2), 139–159. [https://doi.org/10.1016/S0168-1605\(01\)00742-5](https://doi.org/10.1016/S0168-1605(01)00742-5)
- Wainwright, M. (1998). Photodynamic antimicrobial chemotherapy (PACT). *Journal of Antimicrobial Chemotherapy*, 42(1), 13–28. <https://doi.org/10.1093/jac/42.1.13>
- Who. (2015). World Health Organization. WHO estimates of the global burden of foodborne diseases. https://apps.who.int/iris/bitstream/handle/10665/199350/9789241565165_eng.pdf?sequence=1. (Accessed 25 July 2020).
- Żudyte, B., & Luksiene, Z. (2019). Toward better microbial safety of wheat sprouts: Chlorophyllin-based photosensitization of seeds. *Photochemical and Photobiological Sciences*, 18(10), 2521–2530. <https://doi.org/10.1039/c9pp001>